

# FORMATION OF OBSCURING WALLS BY RADIATION FORCE FROM CIRCUMNUCLEAR STARBURSTS AND IMPLICATIONS FOR STARBURST-ACTIVE GALACTIC NUCLEUS CONNECTION

K. OHSUGA AND M. UMEMURA

Center for Computational Physics, University of Tsukuba, Tsukuba, Ibaraki 305-8577, Japan

*Draft version November 26, 2018*

## ABSTRACT

We explore the formation of dusty gas walls induced by a circumnuclear starburst around an active galactic nucleus (AGN). We concentrate our attention on the role of the radiation force by a starburst as well as an AGN, where the effects of optical depth of dusty gas are taken into consideration. First, we solve the hydrostatic equations in spherical symmetry coupled with the frequency-dependent radiative processes, to demonstrate that a geometrically thin, optically thick wall forms due to the radiation pressure by a circumnuclear starburst. Next, in two-dimensional axisymmetric space, we analyze the configuration and the stability of geometrically thin walls which are in balance between radiation pressure and gravity. As a result, it is shown that the radiation force by the circumnuclear starburst works to stabilize optically thick walls surrounding the nucleus. In the case of a brighter starburst with a fainter AGN (e.g.  $L_{\text{SB}}/M_{\text{SB}} \gtrsim 10[L_{\odot}/M_{\odot}]$  and  $L_{\text{AGN}} \lesssim 10^{11}L_{\odot}$ ), there form double walls, an inner one of which is located between the nucleus and the circumnuclear starburst, and an outer one of which enshrouds both the starburst regions and the nucleus. The total extinction of both walls turns out to be larger for a brighter starburst, which is  $A_V \sim 10$  for  $L_{\text{SB}}/M_{\text{SB}} \gtrsim 10^2[L_{\odot}/M_{\odot}]$ . As a consequence, double walls could heavily obscure the nucleus to make the AGN type 2. The outer wall may provide an explanation for the recent indications for large-scale obscuring materials in Seyfert 2's. Also, it is predicted that the AGN type is time-dependent according to the stellar evolution in the starburst, which shifts from type 2 to type 1 in several times  $10^7$  yr owing to the disappearance of walls. In contrast, if the AGN itself is much brighter than the starburst as a quasar is, then neither wall forms regardless of the starburst activity and the nucleus is likely to be identified as type 1. To conclude, the radiatively-supported gas walls could be responsible for the putative correlation between AGN type and the starbursts, whereby Seyfert 2 galaxies are more frequently associated with circumnuclear starbursts than type 1, whereas quasars are mostly observed as type 1 regardless of star-forming activity in the host galaxies.

*Subject headings:* galaxies: active — galaxies: evolution — galaxies: nuclei — galaxies: starburst — quasars: general — radiative transfer

## 1. INTRODUCTION

There has been a good deal of evidence on an obscuring torus of subparsec scale, which surrounds an active galactic nuclei (AGN) (Antonucci 1984; Wilson, Ward, & Haniff 1988; Barthel 1989; Blanco, Ward, & Wright 1990; Miller & Goodrich 1990; Awaki et al. 1991; Storchi-Bergmann, Mulchaey, & Wilson 1992). The obscuring torus is thought to be responsible for the dichotomy of AGN type in the context of the unified model (Antonucci 1993, for a review). However, the origin and physical structure of the torus has not been well elucidated, although some intriguing models are proposed by Krolik & Begelman (1988), Pier & Krolik (1992a, 1992b, 1993), Efstathiou & Rowan-Robinson (1995), and Manske, Henning, & Men'shchikov (1998).

Recent observations on AGN hosts have gradually revealed that the properties of host galaxies of Seyferts are intrinsically unlike between type 1 and type 2 (Heckman et al. 1989; Maiolino et al. 1995, 1997, 1998a; Pérez-Olea & Colina 1996; Hunt et al. 1997; Malkan, Gorjian, & Tam 1998; Storchi-Bergmann, Schmitt, & Fernandes 1999; Storchi-Bergmann et al. 2000; González Delgado, Heckman, & Leitherer 2001). The Seyfert 2 galaxies are more frequently associated with the circumnuclear star-

bursts than type 1's. In contrast, quasars (QSOs) are mostly observed as type 1, although the QSO hosts often exhibit vigorous star-formation activity (Barvainis, Antonucci, & Coleman 1992; Ohta et al. 1996; Omont et al. 1996; Schinnerer, Eckart, & Tacconi 1998; Brotherton et al. 1999; Canalizo & Stockton 2000a, 2000b; Dietrich & Wilhelm-Erkens 2000). [It is noted that the QSO hosts are fainter than QSO nuclei themselves (McLeod & Rieke 1995b; Bahcall et al. 1997; Hooper, Impey, & Foltz 1997; Crawford et al. 1999; Kirhakos et al. 1999; McLure et al. 1999; McLure, Dunlop, & Kukula 2000).] Such correlation with circumnuclear starbursts seems beyond understanding based upon the picture of the unified model where the bifurcation of AGN type is simply accounted for the orientation of the nucleus surrounded by an obscuring torus.

We have some significant pieces of information on the obscuring materials. By X-ray observations, it is indicated that most Seyfert 2 nuclei are heavily obscured along the line of sight with at least  $A_V > 10$  and sometimes  $A_V > 100$  (Matt et al. 1996, 1999; Maiolino et al. 1998b; Bassani et al. 1999; Risaliti, Maiolino, & Salvati 1999). On the other hand,  $A_V$  of the nuclear or circumnuclear regions is estimated to be between a few and several by IR and optical observations (Rix et al. 1990; Roche et al. 1991; Goodrich, Veilleux, & Hill 1994; McLeod & Rieke

1995a; Oliva, Marconi, & Moorwood 1999). Also, it is argued that a component of obscuring materials must be extended up to  $\geq 100$  pc in addition to a compact component confined into subparsec scales (Rudy, Cohen, & Ake 1988; Miller, Goodrich, & Mathews 1991; Goodrich 1995; McLeod & Rieke 1995a; Maiolino et al. 1995; Maiolino & Rieke 1995; Malkan, Gorjian, & Tam 1998). These facts may suggest that the distributions of dusty gas around an AGN are much more diverse than used to be considered, and they have a close relation with circumnuclear starburst events.

Recently, Ohsuga & Umemura (1999, hereafter Paper I) have suggested a novel picture for the starburst-AGN connection, where a large-scale dusty wall of several hundred parsecs is built up due to radiation force by a circumnuclear starburst as well as an AGN. This model provides a possibility that an AGN type is regulated by circumnuclear starbursts, and also it gives a physical origin of extended obscuring materials. However, the dusty wall was analyzed in an optically thin regime. Thus, the possibility of the strong obscuration with  $A_V \gg 1$  is still an open question in this picture.

In this paper, by taking the optical depth of dusty gas into consideration, we consider the effects of radiation force by a circumnuclear starburst as well as an AGN, and investigate the stable configuration of dusty gas. To begin with, we solve hydrostatic equations coupled with the frequency-dependent radiative processes with assuming spherical symmetry. By this analysis, we demonstrate that a geometrically thin, optically thick wall forms due to radiation pressure by a starburst. Next, we obtain the stable equilibrium configuration of dusty gas walls in two-dimensional axisymmetric space. Finally, we attempt to classify the AGN type according to the starburst luminosity and the AGN luminosity. Moreover, taking account of the stellar evolution in starburst regions, we discuss the time evolution of the circumnuclear structure. In §2, the radiation fields and gravitational fields are modeled. In §3, the structure of a dusty wall is analyzed in spherically symmetric approximation, demonstrating that a geometrically thin, optically thick wall can form due to radiation force by a starburst. In §4, the configuration of dusty gas in two-dimensional axisymmetric space is investigated with an approximation of geometrically-thin walls, and the conditions for the wall formation are given. In §5, based upon the present picture, we discuss the implications for the starburst-AGN connection. Furthermore, the evolution of AGN type which is predicted by the formation of the obscuring walls is shown in §6. §7 is devoted to the conclusions.

## 2. RADIATION FIELDS AND GRAVITATIONAL FIELDS

Recent observations have been revealed that the circumnuclear starburst regions frequently exhibit ring-like features (Wilson et al. 1991; Forbes et al. 1994; Marconi et al. 1994; Mauder et al. 1994; Buta, Purcell, & Crocker 1995; Barth et al. 1995; Leitherer et al. 1996; Maoz et al. 1996; Storch-Bergman, Wilson, & Baldwin 1996). Therefore, as a component of radiation sources, we assume a starburst ring whose bolometric luminosity, radius, and total mass are  $L_{\text{SB}}$ ,  $R_{\text{SB}}$ , and  $M_{\text{SB}}$ , respectively. [Even if the starburst regions are localized, the radiation fields

could be equivalent to that by a ring-like source owing to the short rotation timescale (see also Paper I)]. We also include an AGN itself, in which the bolometric luminosity is  $L_{\text{AGN}}$  and we simply assume an energy spectrum of  $L_{\nu}^{\text{AGN}} \propto \nu^{-1}$  between 0.01 eV and 100 keV (Blandford, Netzer, & Woltjer 1990). To calculate the bolometric luminosity and the energy spectrum of the starburst ring, we assume the initial mass function (IMF) to be of Salpeter-type,

$$\phi \propto (m_*/M_{\odot})^{-1.35}, \quad (1)$$

and the star formation rate (SFR) in the starburst regions to be

$$\text{SFR} \propto \exp\left(-\frac{t_{\text{SB}}}{10^7 \text{yr}}\right), \quad (2)$$

where  $t_{\text{SB}}$  is the elapsed time after the initial starburst. The total luminosity is regulated by the mass-luminosity relation,  $(l_*/L_{\odot}) = (m_*/M_{\odot})^{3.7}$ , and the mass-age relation,  $\tau = 1.1 \times 10^{10} \text{yr} (m_*/M_{\odot})^{-2.7}$ , where  $m_*$  and  $l_*$  are respectively stellar mass and stellar luminosity. Here, we consider the mass range of  $2M_{\odot} - 40M_{\odot}$  in the IMF, since several observations indicate that the IMF is deficient in low mass stars with the cutoff of about  $2M_{\odot}$ , and the upper mass limit is inferred to be around  $40M_{\odot}$  (Doyon, Puxley, & Joseph 1992; Charlot et al. 1993; Doane & Mathews 1993; Hill et al. 1994; Brandl et al. 1996). In addition, we employ the mass-temperature relation,  $(T_*/T_{\odot}) = (m_*/M_{\odot})^{0.575}$ , and the energy spectrum of the star is assumed to be the blackbody spectrum with the effective temperature,  $T_*$ . We neglect the radiation from the supernovae, because the long term-averaged luminosity of supernovae is less than 10% of the total stellar luminosity of the ring as shown in Paper I. Resultantly, the bolometric luminosity of the starburst ring is in proportion to the total mass, and decreases with time.

As for the gravitational fields, we should consider the galactic bulge, the central black hole, and the starburst ring. But, the gravitational fields in circumnuclear regions suffer from some uncertainty. Recent observations provide significant information which allows us to model the gravitational fields in circumnuclear regions. For instance, the stellar rotation velocity in the Circinus galaxy (a closest Seyfert 2 galaxy) shows that the mass distributions in circumnuclear regions are not concentrated into a point-like object but extended to a few hundred parsecs (Maiolino et al. 1998a). Therefore, we consider also such an inner bulge-like component. We assume the galactic bulge to be an uniform sphere whose mass and radius are  $M_{\text{GB}}$  and  $R_{\text{GB}}$ , the inner bulge also to be an uniform sphere whose mass and radius are  $M_{\text{IB}}$  and  $R_{\text{IB}}$ , and the mass of the black hole to be  $M_{\text{BH}}$ , respectively.

The observations of IRAS galaxies by Scoville et al. (1991) show that the central regions within kilo parsecs possess the mass of  $\lesssim 10^{10} M_{\odot}$ . This is comparable to a typical mass of galactic bulge. A rotation velocity of a starburst ring also implies that the dynamical mass within a few hundred parsecs is several  $10^9 M_{\odot}$  (Elmouttie et al. 1998), which provides an estimation of the mass of inner bulge. In addition, Maiolino et al. (1998a) estimated an upper limit of a putative black hole as several  $10^6 M_{\odot}$ . (We tentatively assume the black hole of  $10^7 M_{\odot}$ , but the overall results are not changed much even if one

assumes  $M_{\text{BH}} = 10^6 M_{\odot}$  or  $10^8 M_{\odot}$ .) By taking these observational data into account, we adopt the mass ratio as  $M_{\text{GB}} : M_{\text{IB}} : M_{\text{BH}} = 1 : 0.1 : 10^{-3}$ . On the other hand, the mass of the starburst ring,  $M_{\text{SB}}$ , is supposed to be between  $10^7 M_{\odot}$  and  $10^{10} M_{\odot}$ . Also, a starforming ring is observed around a few hundred parsecs in some galaxies (Marconi et al. 1994; Elmouttie et al. 1998). Hence, here we assume a starburst ring at a radius of 200 pc. For the size ratios, we employ  $R_{\text{GB}} : R_{\text{SB}} : R_{\text{IB}} = 5 : 1 : 0.5$ .

### 3. STRUCTURE OF RADIATIVELY-SUPPORTED OBSCURING WALL

The equilibrium configuration of dusty gas is nearly spherically symmetric as shown in the next section. Thus, first we investigate the structure of a radiatively-supported gas wall inside the starburst ring under an approximation of local spherical symmetry. For this purpose, we assume the gravity by the starburst ring to be constant at a part of the wall of interest. Also, the radiation force by the starburst ring is assumed to be a function solely of optical depth measured from the outer surface of the wall. (Rigidly speaking, both assumptions are verified only when the wall is geometrically thin and located at the equatorial plane.) Under these assumptions, we solve the one-dimensional radiation-hydrostatic equation, coupled with ionization process and thermal process.

The radiation-hydrostatic equation is given by

$$-\frac{GM_l}{l^2} - \frac{1}{\rho_g} \frac{dP_g}{dl} + \int \frac{\chi_{\nu}}{c} \frac{L_{\nu}^{\text{AGN}} e^{-\tau_{\nu}}}{4\pi l^2} d\nu + f_{\text{grav}}^{\text{SB}} - \int \frac{\chi_{\nu}}{c} F_{\nu}^{\text{SB}} e^{-(\tau_{\nu}^{\text{total}} - \tau_{\nu})} d\nu = 0, \quad (3)$$

where  $l$  is the radius,  $M_l$  is the total mass within the radius  $l$ ,  $\rho_g$  is the gas density,  $P_g$  is the gas pressure,  $\chi_{\nu}$  is the mass extinction coefficient of dusty gas,  $\tau_{\nu}$  is the optical depth of the wall measured from the center,  $\tau_{\nu}^{\text{total}}$  is the total optical depth of the wall, and  $f_{\text{grav}}^{\text{SB}}$  and  $F_{\nu}^{\text{SB}}$  are respectively the gravity and the radiation flux by the starburst ring. It is noted that  $f_{\text{grav}}^{\text{SB}}$  and  $F_{\nu}^{\text{SB}}$  provide non-spherical components in real situations. The effects of the non-sphericity are taken into consideration by evaluating these quantities by two-dimensional axisymmetric calculations.

Recent observations report the existence of a large amount of dust, molecular gas, and metals in QSOs (Barvainis, Antonucci, & Coleman 1992; Ohta et al. 1996; Omont et al. 1996; Dietrich & Wilhelm-Erkens 2000). Therefore, we suppose the dust-to-gas mass ratio to be 0.03, which is three times as large as that observed in the Solar neighborhood. Since the mass density of dust and Thomson scattering are negligible, the extinction is given by  $\chi_{\nu} = (n_{\text{H}} \chi_{\text{HI}} \sigma_{\nu}^{\text{HI}} + \alpha_{\nu}^{\text{d}}) / \rho_g$ . Here,  $n_{\text{H}}$  is the number density of hydrogen nuclei,  $\chi_{\text{HI}}$  is the fraction of neutral hydrogen,  $\sigma_{\nu}^{\text{HI}}$  is the photoionization cross-section, and  $\alpha_{\nu}^{\text{d}}$  is the absorption coefficient of dust. For the dust model, we employ the grain size distribution as  $n_{\text{d}}(a_{\text{d}}) \propto a_{\text{d}}^{-3.5}$  in a range of  $[0.01 \mu\text{m}, 1 \mu\text{m}]$  (Mathis, Rumpl, & Nordsieck 1977), and absorption cross-section,  $\pi a_{\text{d}}^2 \min[1, (\lambda/2\pi a_{\text{d}})^{-2}]$ , where  $a_{\text{d}}$  is the grain radius, and the density of solid material within a grain is assumed to be  $1.0 \text{g cm}^{-3}$ .

The equation of the ionization balance is

$$\Gamma^{\gamma} \chi_{\text{HI}} + \Gamma^{\text{ci}} n_{\text{H}} \chi_{\text{HI}} (1 - \chi_{\text{HI}}) = \alpha_{\text{rec}} n_{\text{H}} (1 - \chi_{\text{HI}})^2, \quad (4)$$

where  $\Gamma^{\gamma}$  is the photoionization rate,  $\Gamma^{\text{ci}}$  is the collisional ionization rate, and  $\alpha_{\text{rec}}$  is the recombination coefficient.  $\Gamma^{\gamma}$  is given by

$$\Gamma^{\gamma} = \int_{\nu_{\text{L}}} \sigma_{\nu}^{\text{HI}} \left\{ \frac{L_{\nu}^{\text{AGN}} e^{-\tau_{\nu}}}{4\pi l^2} + F_{\nu}^{\text{SB}} e^{-(\tau_{\nu}^{\text{total}} - \tau_{\nu})} \right\} \frac{1}{h\nu} d\nu, \quad (5)$$

with  $\nu_{\text{L}}$  being the Lyman limit frequency, and  $\Gamma^{\text{ci}}$  is  $1.19 \times 10^{-10} T_{\text{g}}^{1/2} \exp(-1.58 \times 10^5 / T_{\text{g}})$  (Sherman 1979). If a free electron recombines directly to ground state of hydrogen, the emitted photon has enough energy to cause further photoionization. Since a part of recombination photons are absorbed by the dust grain, the value  $\alpha_{\text{rec}}$  is given by  $\alpha_{\text{rec}} = \alpha_{\text{A}} - (\alpha_{\text{A}} - \alpha_{\text{B}}) n_{\text{H}} \chi_{\text{HI}} \sigma_{\nu_{\text{L}}}^{\text{HI}} / \rho_{\text{g}} \chi_{\nu_{\text{L}}}$ , where total recombination coefficient,  $\alpha_{\text{A}}$ , is well fitted by  $\alpha_{\text{A}} = 2.1 \times 10^{-13} (T_{\text{g}} / 10^4 \text{K})^{-1/2} \phi(16 T_{\text{g}} / 10^4 \text{K})$ , with  $\phi(y) = 0.5(1.7 + \ln y + 1/6y)$  for  $y \geq 0.5$ , or  $y(-0.3 - 1.2 \ln y) + y^2(0.5 - \ln y)$  for  $y < 0.5$  (Sherman 1979), and the recombination coefficient to all excited levels of hydrogen,  $\alpha_{\text{B}}$ , is approximately related with  $\alpha_{\text{A}}$  as  $\alpha_{\text{B}} = \alpha_{\text{A}} \exp\{-0.487(T_{\text{g}} / 10^4 \text{K})^{1/5}\}$ , where  $T_{\text{g}}$  is the gas temperature.

The equation for the energy balance of the gas is given by

$$\mathcal{H}_{\text{g}}^{\gamma} = \mathcal{L}_{\text{g}}^{\text{rec}} + \mathcal{L}_{\text{g}}^{\text{ff}} + \mathcal{L}_{\text{g}}^{\text{ci}} + \mathcal{L}_{\text{g}}^{\text{ce}} + \mathcal{L}_{\text{g}}^{\text{Z}} + \mathcal{L}_{\text{g}}^{\text{gd}}, \quad (6)$$

where  $\mathcal{H}_{\text{g}}^{\gamma}$  is the heating rate of the gas due to direct radiation by the starburst ring as well as the AGN, and  $\mathcal{L}_{\text{g}}^{\text{rec}}$ ,  $\mathcal{L}_{\text{g}}^{\text{ff}}$ ,  $\mathcal{L}_{\text{g}}^{\text{ci}}$ ,  $\mathcal{L}_{\text{g}}^{\text{ce}}$ ,  $\mathcal{L}_{\text{g}}^{\text{Z}}$ , and  $\mathcal{L}_{\text{g}}^{\text{gd}}$ , are respectively the cooling rates for gas through radiative recombination, free-free emission, collisional ionization, collisional excitation, emission for metal, and collision with dust.  $\mathcal{H}_{\text{g}}^{\gamma}$  is given by

$$\mathcal{H}_{\text{g}}^{\gamma} = \int_{\nu_{\text{L}}} \chi_{\text{HI}} \sigma_{\nu}^{\text{HI}} \left\{ \frac{L_{\nu}^{\text{AGN}} e^{-\tau_{\nu}}}{4\pi l^2} + F_{\nu}^{\text{SB}} e^{-(\tau_{\nu}^{\text{total}} - \tau_{\nu})} \right\} \left(1 - \frac{\nu_{\text{L}}}{\nu}\right) d\nu, \quad (7)$$

where we neglect the energy transfer by the Compton scattering because the timescale is estimated to be  $\sim 10^9$  yr and it is much longer than the typical lifetime of AGN,  $\sim 10^8$  yr, in the circumnuclear regions of  $>$  several 10 pc even in the case of very luminous AGNs with  $\sim 10^{13} L_{\odot}$ .  $\mathcal{L}_{\text{g}}^{\text{rec}}$ ,  $\mathcal{L}_{\text{g}}^{\text{ff}}$ ,  $\mathcal{L}_{\text{g}}^{\text{ci}}$ , and  $\mathcal{L}_{\text{g}}^{\text{ce}}$  are represented by  $\mathcal{L}_{\text{g}}^{\text{rec}} = 3kT_{\text{g}} \alpha_{\text{rec}} n_{\text{H}} (1 - \chi_{\text{HI}})^2 / 2$ ,  $\mathcal{L}_{\text{g}}^{\text{ff}} = 1.42 \times 10^{-27} T_{\text{g}}^{1/2} n_{\text{H}} (1 - \chi_{\text{HI}})^2$ ,  $\mathcal{L}_{\text{g}}^{\text{ci}} = \Gamma^{\text{ci}} h\nu_{\text{L}} n_{\text{H}} \chi_{\text{HI}} (1 - \chi_{\text{HI}})$ ,  $\mathcal{L}_{\text{g}}^{\text{ce}} = 7.5 \times 10^{-19} \exp(-1.18 \times 10^5 / T_{\text{g}}) n_{\text{H}} \chi_{\text{HI}} (1 - \chi_{\text{HI}})$  (Black 1981), and  $\mathcal{L}_{\text{g}}^{\text{Z}} = 4 \times 10^{-28} T_{\text{g}}^{1/2} n_{\text{H}}$  for  $10^2 \text{K} < T_{\text{g}} < 10^4 \text{K}$ , or  $\mathcal{L}_{\text{g}}^{\text{Z}} = 10^{-22.1 - 120Z} T_{\text{g}}^{30Z} n_{\text{H}} - 10^{-22.1} n_{\text{H}}$  for  $10^4 \text{K} < T_{\text{g}} < 10^5 \text{K}$  (Theis, Burkert, & Hensler 1992), where  $Z$  is the metal abundance. Here, the metal abundance is assumed to be  $3Z_{\odot}$ , consistently with the supposed dust-to-gas mass ratio, 0.03. Assuming the collisional equilibrium of charge on a grain, we can estimate  $\mathcal{L}_{\text{g}}^{\text{gd}} = \int n_{\text{d}} \pi a_{\text{d}}^2 da_{\text{d}} \cdot (7 - 6\chi_{\text{HI}}) (8kT_{\text{g}} / \pi m_{\text{p}})^{1/2} (2kT_{\text{g}} - 2kT_{\text{d}})$ , where  $m_{\text{p}}$  is the proton mass and  $T_{\text{d}}$  is the dust temperature. As for the energy balance for dust, the emission from gas is assumed to be absorbed by dust almost on the spot. Then, the energy equation for dust is

$$\mathcal{H}_{\text{d}}^{\gamma} + \mathcal{L}_{\text{g}}^{\text{rec}} + \mathcal{L}_{\text{g}}^{\text{ff}} + \mathcal{L}_{\text{g}}^{\text{ce}} + \mathcal{L}_{\text{g}}^{\text{Z}} + \mathcal{L}_{\text{g}}^{\text{gd}} = \mathcal{L}_{\text{d}}^{\gamma}, \quad (8)$$

where  $\mathcal{H}_d^\gamma$  and  $\mathcal{L}_g^{\text{rec}}$  are the heating rates for dust due to the direct radiation from a starburst ring as well as an AGN and due to the recombination photons from hydrogen, and  $\mathcal{L}_d^\gamma$  is the cooling by dust emission. (This assumption is justified by the fact that a resultant gas wall is optically thick due to dust opacity.)  $\mathcal{H}_d^\gamma$  is given by

$$\mathcal{H}_d^\gamma = \frac{1}{n_{\text{H}}} \int \alpha_\nu^{\text{d}} \left\{ \frac{L_\nu^{\text{AGN}} e^{-\tau_\nu}}{4\pi l^2} + F_\nu^{\text{SB}} e^{-(\tau_\nu^{\text{total}} - \tau_\nu)} \right\} d\nu, \quad (9)$$

$\mathcal{L}_g^{\text{rec}}$  is written as  $\mathcal{L}_g^{\text{rec}} = (3kT_g/2 + h\nu_L)\alpha_{\text{rec}}n_{\text{H}}(1 - \chi_{\text{HI}})^2$ , and  $\mathcal{L}_d^\gamma$  is presented by  $\mathcal{L}_d^\gamma = (\sigma\alpha_{\nu_0}^{\text{d}}/\pi n_{\text{H}})\{\Gamma(6)\zeta(6)/\Gamma(4)\zeta(4)\}(k/h\nu_0)^2 T_d^6$ , where  $\Gamma$  and  $\zeta$  are respectively the gamma function and Riemann's function (Nakamoto & Nakagawa 1994). We note that dust is primarily heated by the direct radiation, so that the dust temperature is not affected heavily even if the heating by the gas emission is dismissed. Moreover, since the absorption cross-section against IR radiation re-emitted from dust is much smaller than that against optical or UV radiation, we suppose that dust grains work as pure absorbers.

The above equations and the equation of state for ideal gas are solved to give the gas density, the gas temperature, the fraction of neutral hydrogen, and the dust temperature as functions of radii. The resultant profile of hydrogen number density and  $A_V$  measured from the center are shown in Figure 1. Here,  $L_{\text{AGN}} = 10^{10}L_\odot$ ,  $M_{\text{SB}} = 10^9M_\odot$ , and  $L_{\text{SB}} = 8.3 \times 10^{10}L_\odot$  ( $t_{\text{SB}} = 3 \times 10^7$  yr) are assumed. As seen in this figure, there forms an optically-thick wall, where the inner surface is pushed outward by the radiation force by the AGN against the gravity by the inner

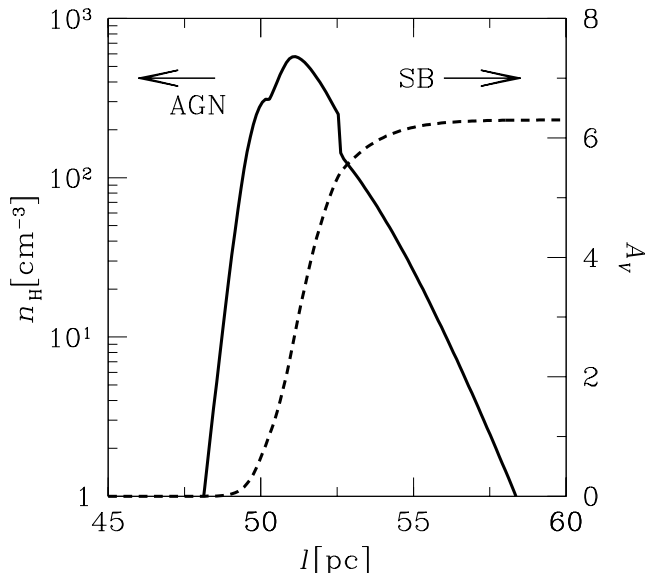


FIG. 1.— The profile of hydrogen number density and the visual extinction  $A_V$  measured from the center are shown as functions of radii,  $l$ . Here,  $L_{\text{AGN}} = 10^{10}L_\odot$ ,  $M_{\text{SB}} = 10^9M_\odot$ , and  $L_{\text{SB}} = 8.3 \times 10^{10}L_\odot$  ( $t_{\text{SB}} = 3 \times 10^7$  yr) are assumed. The AGN is located at the center,  $l = 0$ , and the size of the starburst ring is assumed to be 200 pc. The interior and exterior surface of the wall are irradiated by the radiation from the AGN and the starburst ring, respectively. The density gradient is very steep since the wall is compressed due to strong radiation force by the starburst ring as well as the AGN. The effective thickness of the wall is less than 10% of its radial extension. This figure shows that a geometrically thin, optically thick wall forms.

bulge and the radiation force by the starburst shoves the wall inward. The optical depth ( $A_V$ ) is basically determined by the ratio of the net radiation force to the total gravity if both AGN and starburst are super-Eddington respectively to  $M_l$  and to  $M_{\text{SB}}$ . The density profile of the wall has a peak at  $\sim 50$  pc and the density gradients on both sides of a peak are very steep. Then, the geometrical thickness of the wall is basically determined by the ratio of the square of sound speed to the total radiation force. The gas temperature is around  $10^4\text{K}$  due to the photoheating. As a result, the effective thickness of the wall is less than 10% of its radial extension. Hence, it is concluded that a radiatively-supported wall can be optically thick and geometrically thin. If the starburst is more luminous, the wall would be thinner because the density gradient would be steeper owing to the radiation force. On the other hand, if the mass of the starburst ring is less than  $10^9M_\odot$ , the density profile would be roughly the same, since the force fields are mainly determined by the AGN and the inner bulge. In this analysis it has turned out that the radiation force from the AGN as well as the starburst is exerted mainly on dust. Therefore, for the mass extinction of the dusty gas, we take only the dust opacity into account in two-dimensional calculations below.

Although we have considered the structure of a gas wall inside the starburst ring, the structure of an outer wall beyond the starburst ring can be understood by a similar argument. If an outer wall forms at several hundred parsecs, the photoheating does not work effectively to raise the temperature  $\sim 10^4\text{K}$ , but it becomes around  $\sim 10^2\text{K}$ . Then, the thickness of the wall is much thinner than the inner wall. As for the optical depth ( $A_V$ ), it is determined basically by the ratio of the radiation force to the total gravity for super-Eddington luminosity, and therefore could be  $A_V \gg 1$ .

#### 4. CONFIGURATION OF OBSCURING WALLS

In this section, we examine the equilibrium configuration of a gas wall and the stability in two-dimensional axisymmetric space. We assume the wall to be geometrically thin as analyzed in the previous section. Under the assumption, taking the effects by the optical depth into account, we calculate the radiation force and the gravity which are exerted on a dusty wall. The radiative flux force by the starburst ring is given by

$$f_{\text{SB}}^i = \int \frac{\bar{\chi}_{\text{SB}}}{c} \frac{\rho_{\text{SB}}}{4\pi l_{\text{SB}}^2} \frac{1 - \exp(-\tau_{\text{SB}}/\cos\theta_{\text{SB}})}{\tau_{\text{SB}}/\cos\theta_{\text{SB}}} n^i dV, \quad (10)$$

at a point of  $(r, z)$  in cylindrical coordinates, where  $i$  denotes  $r$  or  $z$ ,  $\bar{\chi}_{\text{SB}}$  is the flux mean mass extinction coefficient averaged over the starburst radiation,  $\tau_{\text{SB}}$  is the total optical depth of the wall which is estimated with using  $\bar{\chi}_{\text{SB}}$ ,  $\rho_{\text{SB}}$  is the luminosity density in the starburst ring,  $l_{\text{SB}}$  is the distance from  $(r, z)$  to a volume element  $dV$  of the ring,  $\theta_{\text{SB}}$  is the viewing angle from this element, and  $n^i$  is the directional cosine. Similarly, the radiative flux force by the AGN is presented by

$$f_{\text{AGN}}^i = \frac{\bar{\chi}_{\text{AGN}}}{c} \frac{L_{\text{AGN}}}{4\pi l^2} \frac{1 - \exp(-\tau_{\text{AGN}}/\cos\theta_{\text{AGN}})}{\tau_{\text{AGN}}/\cos\theta_{\text{AGN}}} \frac{i}{l}, \quad (11)$$

at the same point, where  $\bar{\chi}_{\text{AGN}}$  is the flux mean mass extinction averaged over the AGN radiation,  $l$  is the distance,  $\theta_{\text{AGN}}$  is the viewing angle from the center, and  $\tau_{\text{AGN}}$  is the

total optical depth, which is estimated with using  $\bar{\chi}_{\text{AGN}}$ . Using equations (10) and (11), the equilibrium between the radiation force and the gravity is determined by

$$-\frac{d\Phi}{dz} = f_{\text{SB}}^z + f_{\text{AGN}}^z + f_{\text{grav}}^z = 0, \quad (12)$$

in the vertical directions ( $z$ -directions) and

$$-\frac{d\Phi}{dr} = \frac{j^2}{r^3} + f_{\text{SB}}^r + f_{\text{AGN}}^r + f_{\text{grav}}^r = 0, \quad (13)$$

in the radial directions ( $r$ -directions), where  $\Phi$  is the effective potential,  $j$  is the specific angular momentum of the dusty gas and  $f_{\text{grav}}^i$  is the gravitational force. Furthermore, stable configuration should satisfy the conditions

$$\frac{d^2\Phi}{dz^2} > 0, \quad (14)$$

and

$$\frac{d^2\Phi}{dr^2} > 0. \quad (15)$$

#### 4.1. Inner Obscuring Wall

First, we consider the formation of a dusty wall inside the starburst ring. The wall is irradiated outward by the AGN and inward by the starburst ring. In Figure 2, the resultant equilibrium branches are shown in the  $r$ - $z$  space for  $A_V = 3, 5,$  and  $7$ . Here,  $L_{\text{AGN}} = 10^{10} L_{\odot}$ ,  $M_{\text{SB}} = 10^9 M_{\odot}$ , and  $L_{\text{SB}} = 8.3 \times 10^{10} L_{\odot}$  ( $t_{\text{SB}} = 3 \times 10^7$  yr) are assumed. On each curve, the conditions for stable equilibrium in the vertical directions [(12) and (14)] are satisfied. However, the dashed curves do not satisfy the force balance (13) in the radial directions, so that the dusty gas is likely to be swung away around the curves because of centrifugal force. As a result, it is found that the solid curves are the stable equilibrium branches in both vertical and radial directions, which provide the final configuration of the inner obscuring wall. It is noted that the starburst ring plays an important role for the force balance and the stability of the wall. The AGN as well as the bulge components provides only spherically symmetric forces, whereas the radiation force and the gravity by the starburst ring are not spherically symmetric. Therefore, on the tangential plane, the azimuthal component of centrifugal force can balance only with that of radiation force by the ring (see Figure 3). To realize this situation, the starburst luminosity is required to be super-Eddington,  $L_{\text{SB}} > 4\pi cGM_{\text{SB}}/\bar{\chi}_{\text{SB}}$ . Since the effective radiation force by the starburst ring is weakened for a large viewing angle  $\theta_{\text{SB}}$ , the radial balance breaks down in the vicinity of the rotation axis ( $z$ -axis).

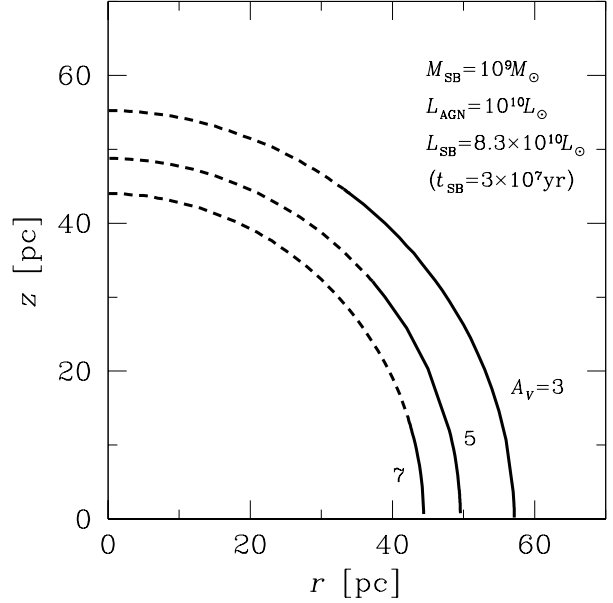


FIG. 2.— Equilibrium configuration of inner walls is shown in  $r$ - $z$  space for  $A_V = 3, 5,$  and  $7$ . Here,  $L_{\text{AGN}} = 10^{10} L_{\odot}$ ,  $M_{\text{SB}} = 10^9 M_{\odot}$ , and  $L_{\text{SB}} = 8.3 \times 10^{10} L_{\odot}$  ( $t_{\text{SB}} = 3 \times 10^7$  yr) are assumed. The solid curves represent the stable branches, while the dashed curves are radially nonequilibrium branches. The solid curves show the final configuration of stable inner walls. Since the effective radiation force by the ring is weakened in the vicinity of the rotation axis in the case of the inner wall due to a large viewing angle, an opening forms and it is shown by a dashed curve.

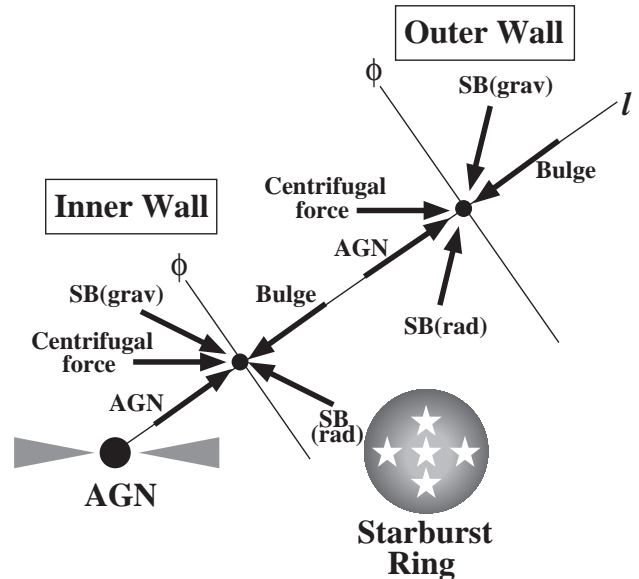


FIG. 3.— Schematic edge-on sketch showing the forces exerted on the inner wall as well as the outer wall. Arrows represent the orientations of forces, although the lengths of the arrows do not correspond to the strength of forces. As a result of numerical calculation, it is found that the starburst ring provides nonspherical radiation force and gravity, whereas the forces by the AGN as well as the bulge components are spherically symmetric. Hence, the walls form if the azimuthal ( $\phi$ ) component of radiation force by the starburst ring balances with that of total force of the gravity by the ring and the centrifugal force.

An opening grows as the optical depth ( $A_V$ ) increases, because of the dilution of the effective radiation force by the ring [see equation (10)]. In order that a stable inner wall enshrouds the nuclear regions with a large covering factor

(opening angle  $< 90^\circ$ ),  $A_V$  is constrained from above as

$$A_V \lesssim \frac{\chi_V L_{SB}}{4\pi c G M_{SB}}, \quad (16)$$

where  $\chi_V$  is the mass extinction at the  $V$  band. On the other hand, the radiation force by a very luminous AGN could blow the dusty gas away from the inner bulge regions if the optical depth is not enough to dilute the radiation force. This provides a lower bound of  $A_V$  as

$$A_V > \frac{\chi_V L_{AGN}}{4\pi c G (M_{IB} + M_{BH})}. \quad (17)$$

Because of the time dependence of starburst luminosity, the upper bound of  $A_V$  given by inequality (16) is a decreasing function of time. For a given model, the allowed range of  $A_V$  of the inner wall is presented in the Figure 4 as a function of time,  $t_{SB}$ . In the shaded regions, no

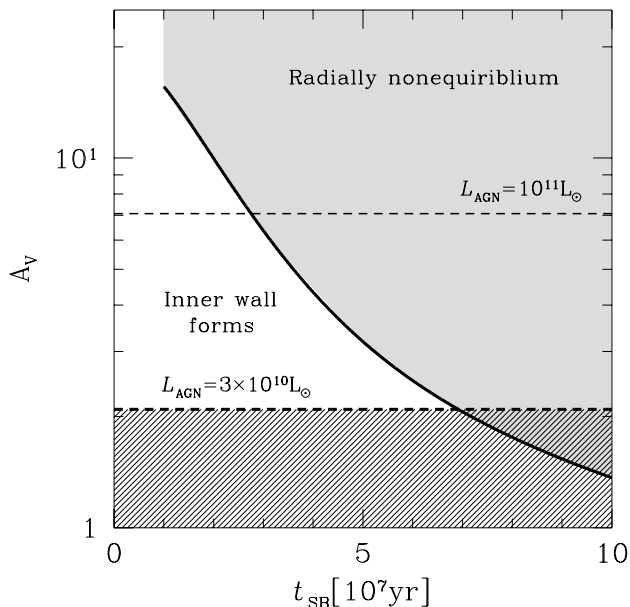


FIG. 4.— The range of  $A_V$  allowed for the inner wall formation. In the shaded area,  $A_V$  does not satisfy the inequality (16), so that the greater part of the wall is out of radial equilibrium. Also, the dusty gas is blown away due to strong radiation force by the AGN in the hatched area in the case of  $L_{AGN} = 3 \times 10^{10} L_\odot$ .

stable equilibrium branches with a large covering factor exist and in the hatched regions the radiation force by the AGN blows out the dusty gas. If the upper bound in (16) is smaller than the lower bound in (17), there is no allowed value for  $A_V$ . That is to say, no inner wall forms regardless of  $t_{SB}$  if

$$L_{AGN} > (M_{IB} + M_{BH}) \frac{L_{SB}}{M_{SB}}. \quad (18)$$

#### 4.2. Outer Obscuring Wall

Next, we investigate the formation of an outer wall with the radial extension of  $\geq R_{SB}$ . In Figure 5, the resultant equilibrium branches of the outer wall are shown in the  $r$ - $z$  plane. As shown in this figure, a nearly spherical wall forms. In this case, the starburst ring as well as the AGN irradiate the inside of the wall. Therefore, the radiation force by the starburst ring is exerted outward

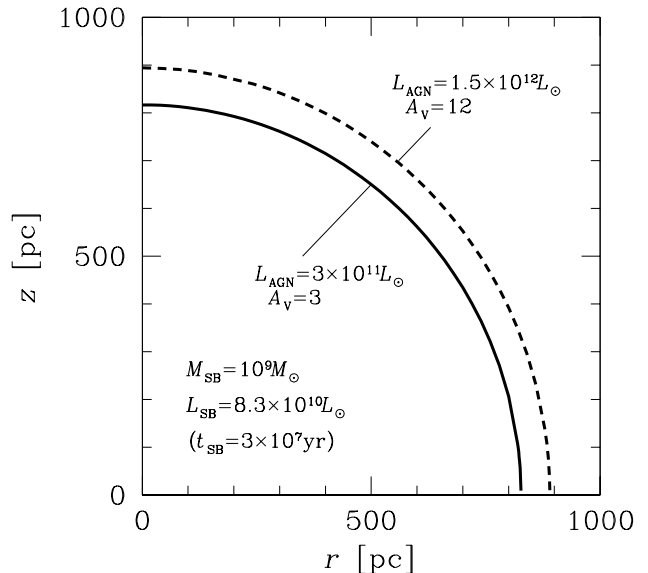


FIG. 5.— Equilibrium configuration of an outer wall beyond the starburst regions is shown in  $r$ - $z$  space for two cases of the AGN luminosity, say,  $L_{AGN} = 3 \times 10^{11} L_\odot$  and  $1.5 \times 10^{12} L_\odot$ . Here,  $M_{SB} = 10^9 M_\odot$  and  $L_{SB} = 8.3 \times 10^{10} L_\odot$  are assumed. The solid curves represent stable branches, while the dashed curves are radially nonequilibrium branches. The outer wall is roughly of spherical shape and covers a wide solid angle whenever it forms.

on the dusty wall, although the inner wall is pushed inward by the starburst radiation. But, it has been found by the present analyses that the radial equilibrium and stable condition for the outer wall formation is again given by the inequality (16) for a wide range of parameters. It is also required that the starburst ring is super-Eddington. This can be also understood by the argument of force balance in the azimuthal directions at a point on the wall. The azimuthal component of the centrifugal force can be balanced only by the force by the starburst ring, because only the starburst ring provides a spherical force (see Figure 3). The upper value of the allowed  $A_V$  decreases again with time as the starburst becomes dimmer. As a prerequisite condition for the formation of the wall,  $(\bar{\chi}_{AGN} L_{AGN} + \bar{\chi}_{SB} L_{SB}) / 4\pi c G (M_{SB} + M_{IB} + M_{BH}) > 1$  is required, otherwise the dusty gas is not held at the regions of  $> R_{IB}$  even in the case of an optically-thin wall. Since the radiation force is diluted by the optical depth of the wall, the upper bound of  $A_V$  is provided as

$$A_V < \frac{\chi_V (L_{AGN} + L_{SB})}{4\pi c G (M_{SB} + M_{IB} + M_{BH})}, \quad (19)$$

for the sustainment of the dusty gas. On the other hand, the lower bound of  $A_V$  is estimated by

$$A_V > \frac{\chi_V (L_{AGN} + L_{SB})}{4\pi c G (M_{GB} + M_{SB} + M_{IB} + M_{BH})}, \quad (20)$$

since the radiation force would blow out the dusty gas in most regions if the  $A_V$  of the wall is smaller than this value. Comparing this lower limit to equation (16), we find that no outer wall forms if the AGN luminosity satisfies the inequality as

$$L_{AGN} > (M_{GB} + M_{IB} + M_{BH}) \frac{L_{SB}}{M_{SB}}. \quad (21)$$

It is noted that this condition involves the prohibition condition (18) for an inner wall.  $A_V$  is limited from above as

$$A_V < \min \left[ \frac{\chi_V L_{SB}}{4\pi c G M_{SB}}, \frac{\chi_V (L_{AGN} + L_{SB})}{4\pi c G (M_{SB} + M_{IB} + M_{BH})} \right]. \quad (22)$$

### 5. IMPLICATIONS FOR STARBURST-AGN CONNECTION

From a viewpoint of the formation of radiatively-supported obscuring walls, we discuss the connection between the AGN type and the starburst events. Based upon the conditions of (18) and (21), in Figure 6 the prediction for the wall formation is summarized in a diagram of  $L_{AGN}$  versus  $L_{SB}/M_{SB,9}$ , where  $M_{SB,9}$  is the mass of a starburst in units of  $10^9 M_\odot$ . An outer wall forms below a solid line and an inner wall as well as an outer wall forms below a dashed line. A vertical dot-dashed line shows the boundary for the formation of the walls. The possible values of  $A_V$  are also shown by thin dot-dashed lines. Here, it is stressed that the possible  $A_V$  is practically determined by equation (22) for the outer wall. However, if the mass supply to an altitude of several 100 pc by a superbubble driven by a circumnuclear starburst is insufficient, no outer wall of  $A_V \gtrsim$  several might form (see next section). The figure shows that for a luminous starburst and a relatively faint AGN, both inner and outer walls are built up, and

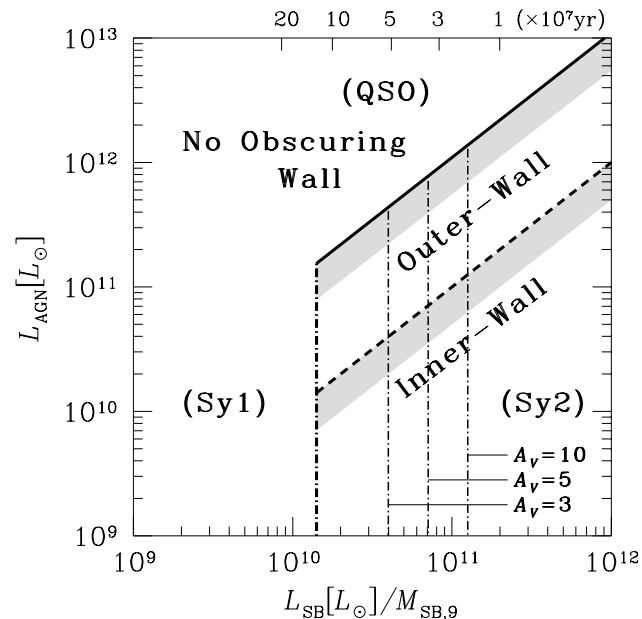


FIG. 6.— The conditions for the formation of obscuring walls are shown in a diagram of the AGN luminosity  $L_{AGN}$  versus the starburst luminosity  $L_{SB}$ , where the starburst luminosity is divided by the mass of starburst in units of  $10^9 M_\odot$ . An outer wall forms below a solid line and an inner wall as well as an outer wall forms below a dashed line. A vertical dot-dashed line gives the boundary for the formation of the walls based on the condition that the starburst is super-Eddington, and the specific values of  $A_V$  are also shown by thin dot-dashed lines. The figure shows that for a luminous starburst and a relatively faint AGN, the nucleus is enshrouded by double walls with the total extinction of  $A_V > 10$ , and therefore it is likely to be identified as a type 2 AGN (Sy 2). If a starburst is intrinsically faint or becomes dimmer owing to the stellar evolution, neither wall forms and the nucleus is observed as a type 1 AGN (Sy 1). The age of the starburst based on the present stellar evolution model is shown in the upper abscissa. Furthermore, if the AGN is much more luminous, the wall formation is prohibited regardless of the starburst luminosity (QSO).

the nucleus could be obscured with the total extinction of  $A_V \sim 10$ . Then, the nucleus is likely to be identified as a type 2 AGN (Sy 2). Also, the outer wall may be consistent with the recently observed obscuring material extending up to  $\geq 100$  pc around the nuclei (Rudy, Cohen, & Ake 1988; Miller, Goodrich, & Mathews 1991; Goodrich 1995; McLeod & Rieke 1995a; Maiolino et al. 1995; Maiolino & Rieke 1995; Malkan, Gorjian, & Tam 1998).

By X-ray observations, the  $A_V$  of most Seyfert 2 nucleus is estimated to be  $> 10$  and sometimes  $> 100$ . Such a difference between  $A_V$  estimated by the X-ray observations and  $A_V$  assessed by the IR or Optical observations might be due to obscuring matter free from dust, located just inside the dust sublimation radius of subparsec. The structure and formation mechanism of obscuring material in subparsec regions is debatable, but it is beyond the scope of this paper.

If a starburst is intrinsically faint, neither an outer wall nor inner one is expected to form. Then, the nucleus could be observed as a type 1 AGN (Sy 1). These results provide a physical explanation for the putative correlation between AGN type and host properties whereby Seyfert 2 galaxies are more frequently associated with circumnuclear starbursts than type 1 galaxies. In the cases of the moderate extinction by the walls may lead to intermediate types of AGNs, that is, type 1.9, 1.8, 1.5, or 1.2 according to the decrease of the extinction.

In addition, we have come to a significant conclusion that a much higher AGN activity as (21) would preclude either wall from forming. Then the nucleus tends to be identified as type 1 regardless of the starburst luminosity. This result may be closely related to the fact that QSOs are mostly observed as type 1 regardless of star-forming activity in the host galaxies.

### 6. AGN EVOLUTION

In the previous section, it is shown that the obscuring walls form in the case of the luminous starburst and the relatively faint AGN. It implies that the obscuration of the AGN is time-dependent, since the bolometric luminosity of the starburst ring decreases with time due to stellar evolution. In this section, we discuss the evolution of the AGN type predicted by this picture. The schematic view of the evolution of circumnuclear structure is shown in Figure 7.

In an early evolutionary stage, a large amount of dusty gas could be blown out by superbubbles in the circumnuclear starburst regions. Shapiro & Field (1976), Tomisaka & Ikeuchi (1986), and Norman & Ikeuchi (1989) have shown that a superbubble of  $\sim 1$  kpc powered by massive OB associations forms. As an observational example, the superbubble of 1.1 kpc is observed in the immediately east of the nucleus of nearby Seyfert 2/LINER galaxy NGC3079 (Veilleux et al. 1994).

Also, if the mass supply rate given by Norman & Ikeuchi (1989) is applied to the case of circumnuclear starbursts of  $M_{SB} \sim 10^9 M_\odot$ , the rate into the regions of several 100 pc height from the circumnuclear molecular disk due to superbubbles is estimated as several  $\times 10 M_\odot \text{ yr}^{-1}$ . In the case of the superbubble of the NGC3079, Duric & Seaquist (1988) and Veilleux et al. (1994) evaluated the mass supply rate to be  $\gtrsim 10 M_\odot \text{ yr}^{-1}$  and  $\sim 7 M_\odot \text{ yr}^{-1}$ , respectively. As a

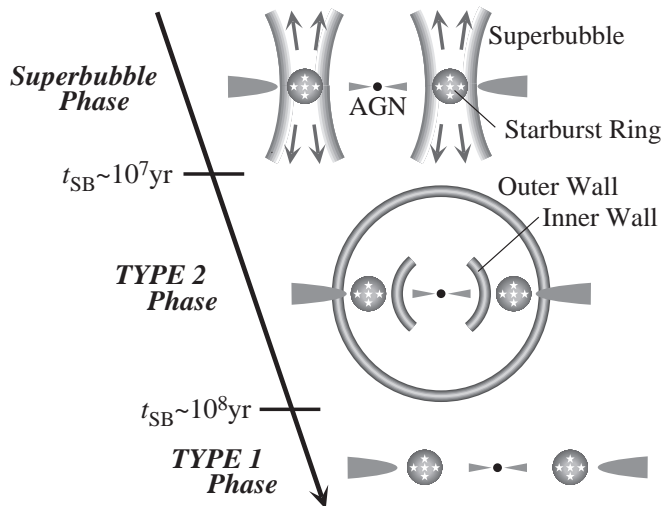


FIG. 7.— Schematic illustration of the evolution of circumnuclear structure. Within  $\sim 10^7$  yr, a large amount of dusty gas is blown away due to superbubbles powered by type II supernovae in circumnuclear starburst regions. The ejected dusty gas is supported by the radiation force by the AGN as well as the starburst ring, and composes the obscuring walls. Then, the nucleus is obscured by both walls and tends to be identified as type 2 AGN (Sy 2). Based on the present stellar evolution model, the nucleus tends to be observed as type 2 AGN (Sy 2) within several  $\times 10^7$  yr, since the possible  $A_V$  decreases with time due to stellar evolution. Finally, the walls disappear and the nucleus are observed as type 1 AGN (Sy 1). Therefore, the AGN is destined to shift from type 2 to type 1 in several times  $10^7$  yr in this picture. However, QSOs are observed as type 1 AGN regardless of the age of the starburst, because the luminous AGN prevent the formation of the walls.

result, the dusty gas of  $\gtrsim 10^8 M_\odot$  would be supplied within a typical lifetime of a superbubble ( $\sim 10^7$  yr) and composes the obscuring walls in the next stage. However, an outer obscuring wall with  $A_V \gtrsim 10$  may not form, because it requires the dusty gas of  $\gtrsim 10^8 M_\odot$ . On the other hand, the required mass for an inner wall is merely  $\sim 10^6 M_\odot$ . The formation timescales of an inner wall and that of an outer wall are several  $\times 10^5$  yr and several  $\times 10^6$  yr, respectively. Both timescales are shorter than the evolutionary timescale of the starburst on the order of  $\sim 10^7$  yr. Thus, the nucleus is likely to be obscured by the inner wall with  $A_V \gtrsim$  several as well as the outer wall with  $A_V \lesssim$  a few, whereas the possible  $A_V$  decreases with time due to the stellar evolution in the starburst regions. Based on the present stellar evolution model, the nucleus is heavily obscured and tends to be observed as type 2 AGN (Sy 2) within several  $\times 10^7$  yr. Also, the inner wall would not be destroyed even if the superbubbles occur in this stage, since the bubble diameter on the equatorial plane is comparable to the scale height of the molecular disk (Schiano 1985; Mac Low & McCray 1988; Tomisaka & Ikeuchi 1988; Mac Low, McCray, & Norman 1989).

In the final stage, the obscuring walls disappear due to the diminution of the bolometric luminosity of the circumnuclear starburst. Then, the nucleus would be identified as type 1 AGN (Sy 1). To conclude, the AGN type is time-dependent and is destined to shift from type 2 to type 1 in several times  $10^7$  yr. It is stressed that no obscuring wall forms in the case of the luminous AGN like QSOs so that type of QSO does not vary, and which is observed as type 1 regardless of the age of the starburst.

Here we have assumed that AGN activity and the cir-

cumnuclear starbursts are simultaneous events. From an observational point of view, it seems to be reasonable, because it is revealed that AGN events are frequently accompanied by starbursts in a variety of data (Scoville et al. 1986; Soifer et al. 1986; Heckman et al. 1989, 1995; Marconi et al. 1994; Neff et al. 1994; Cid Fernandes & Terlevich 1995; Genzel et al. 1995; Maiolino et al. 1995, 1998a; Oliva et al. 1995; Storchi-Bergmann et al. 1996; Rodriguez-Espinosa, Rudy & Jones 1987; Elmouttie et al. 1998; Cid Fernandes, Storchi-Bergmann, & Schmitt 1998). In addition, as a physical solution which links the two events, Norman & Scoville (1988) have suggested a model, whereby the interstellar medium which is released by post-main-sequence stars in starburst regions feeds a central black hole. Also, the radiatively driven mass accretion onto a black hole due to the radiation drag, which is proposed by Umemura, Fukue, & Mineshige (1997, 1998), Fukue, Umemura, & Mineshige (1997), and Ohsuga et al. (1999), would link the two events.

In the present analysis, we have assumed the interstellar gas containing a large amount of dust which is inferred in QSOs (Barvainis, Antonucci, & Coleman 1992; Ohta et al. 1996; Omont et al. 1996; Dietrich & Wilhelm-Erkens 2000). However, the dust grains could be destroyed in shock-heated hot gas and they could be reproduced in cooled superbubble winds. The dust properties around AGNs are under debate also from an observational point of view. The destruction, formation, and growth of the dust grains would make obviously significant effects not only in the present picture but also in a generic problem of obscuration. Thus, this issue should be considered more carefully in the future analysis.

Finally, we discuss the stabilities of the obscuring walls. First of all, the walls are unlikely to be subject to the Rayleigh-Taylor instability. As shown in Figure 1, the density gradient of the inner wall is positive inside the density peak and negative outside the peak. As shown in Figure 3, the acceleration works in the same directions as the density gradient in both sides. Thus, the Rayleigh-Taylor instability does not occur at the inner wall. In the case of the outer wall, the radiation force by the AGN and the starburst ring, which pushes up the wall, is the dominant force at the inner surface, but the dusty gas is attracted by the gravity at the outer surface. As a result, both walls turn out to be stable to the Rayleigh-Taylor mode. However, the walls might be subject to the other instabilities. When the density perturbations occur in the walls, the thick parts of the walls go down by the gravity, whereas the radiation force lifts the less thick parts, since the radiation force is ineffective for heavily optically-thick parts. Then, the walls are likely to have more complicated configurations. Moreover, thermal instabilities might break out, because the radiative cooling works at the dense regions effectively, whereas the gas remains as warm as  $\sim 10^4$  K in the optically thin regions due to radiative heating. Simultaneously, the self-gravitating instability might grow at the cool and dense parts of the walls. Also, the actual circumnuclear starburst is not perfectly ring-shaped but more or less clumpy and therefore makes non-axisymmetric radiation fields, although the wheel effects by the rotation could smear out non-axisymmetric effects to some degree (see also Ohsuga & Umemura 1999). In addition, the dusty walls are pos-



sibly damaged due to the collision of starburst winds or dusty gas expelled from mass losing stars inside the walls. Consequently, the walls could be distorted and fragment into small pieces. How the gas clouds resulting from the fragmentation obscure the AGN is an interesting issue, but the details are not clear before radiation-hydrodynamical simulations are performed.

## 7. CONCLUSIONS

In the present analysis, by taking optical depth due to dust opacity into consideration, we have analyzed the stable equilibrium configuration of dusty gas in the circumnuclear regions in radiation fields by a starburst and an AGN. It has been found that the radiation pressure by a circumnuclear starburst sustains an inner obscuring wall of several ten parsecs and an outer obscuring wall of several hundred parsecs. The total extinction of the obscuring walls has turned out to be around ten. Then, the nucleus would be identified as type 2. If a starburst is intrinsically faint or becomes dimmer owing to the stellar evolution there, neither an outer wall nor inner one would not form. Then, the nucleus could be observed as a type 1 AGN (Sy 1). The results on outer and inner walls share a certain similarity in that the strong radiation force by the AGN

prevents the formation of an outer wall as well as an inner wall. These results provide a physical explanation for the correlation between AGN type and host properties, whereby Seyfert type 2 galaxies are more frequently associated with circumnuclear starbursts than type 1 galaxies, whereas QSOs are mostly observed as type 1 even though vigorous star-forming activities are often observed in the host galaxies. Also, the large-scale outer wall of several hundred parsecs is consistent with the observations on obscuring material extending up to  $\geq 100$  pc around the nuclei. Finally, this model predicts the time evolution of the AGN type from type 2 to type 1 in several times  $10^7$  yr as a circumnuclear starburst becomes dimmer due to stellar evolution.

We are grateful to T. Nakamoto, and H. Susa, for helpful discussion. We thank also the anonymous referee for valuable comments. The calculations were carried out at Center for Computational Physics in University of Tsukuba. This work is supported in part by Research Fellowships of the Japan Society for the Promotion of Science for Young Scientists, 6957 (KO) and the Grants-in Aid of the Ministry of Education, Science, Culture, and Sport, 09874055 (MU).

## REFERENCES

- Antonucci, R. R. J. 1984, *ApJ*, 278, 499  
Antonucci, R. 1993, *ARA&A*, 31, 473  
Awaki, H., Koyama, K., Inoue, H., & Halpern, J. P. 1991, *PASJ*, 43, 195  
Bahcall, J. N., Kirhakos, S., Saxe, D. H., & Schneider, D. P. 1997, *ApJ*, 479, 642  
Barth, A. J., Ho, L. C., Filippenko, A. V., & Sargent, W. L. W. 1995, *AJ*, 110, 1009  
Barthel, P. D. 1989, *ApJ*, 336, 601  
Barrvainis, R., Antonucci, R., & Coleman, P. 1992, *ApJ*, 399, L19  
Bassani, L., Dadina, M., Maiolino, R., Salvati, M., Risaliti, G., della Ceca, R., Matt, G., & Zamorani, G. 1999, *ApJS*, 121, 473  
Black, J. H. 1981, *MNRAS*, 197, 553  
Blanco, P. R., Ward, M. J., & Wright, G. S. 1990, *MNRAS*, 242, 4  
Blandford, R. D., Netzer, H., & Woltjer, L. 1990, *Active Galactic Nuclei* (Berlin: Springer)  
Brandl, B., Sams, B. J., Bertoldi, F., Eckart, A., Genzel, R., Drapatz, S., Hofmann, R., Loewe, M., & Quirrenbach, A. 1996, *ApJ*, 466, 254  
Brotherton, M. S., van Breugel, W., Stanford, S. A., Smith, R. J., Boyle, B. J., Miller, L., Shanks, T., Croom, S. M., & Filippenko, A. V. 1999, *ApJ*, 520, L87  
Buta, R., Purcell, G. B., & Crocker, D. A. 1995, *AJ*, 110, 1588  
Canalizo, G. & Stockton, A. 2000a, *ApJ*, 528, 201  
Canalizo, G. & Stockton, A. 2000b, *AJ*, 120, 1750  
Charlot, S., Ferrari, F., Mathews, G. J., & Silk, J. 1993, *ApJ*, 419, L57  
Cid Fernandes, R., Storchi-Bergmann, T., & Schmitt, H. R. 1998, *MNRAS*, 297, 579  
Cid Fernandes, R. & Terlevich, R. 1995, *MNRAS*, 272, 423  
Crawford, C. S., Lehmann, I., Fabian, A. C., Bremer, M. N., & Hasinger, G. 1999, *MNRAS*, 308, 1159  
Dietrich, M. & Wilhelm-Erkens, U. 2000, *A&A*, 354, 17  
Doane, J. S., & Mathews, W. G. 1993, *ApJ*, 419, 573  
Doyon, R., Puxley, P. J., & Joseph, R. D. 1992, *ApJ*, 397, 117  
Duric, N. & Seaquist, E. R. 1988, *ApJ*, 326, 574  
Efstathiou, A. & Rowan-Robinson, M. 1995, *MNRAS*, 273, 649  
Elmouttie, M., Koribalski, B., Gordon, S., Taylor, K., Houghton, S., Lavezzi, T., Haynes, R., & Jones, K. 1998, *MNRAS*, 297, 49  
Forbes, D. A., Norris, R. P., Williger, G. M., & Smith, R. C. 1994, *AJ*, 107, 984  
Fukue, J., Umemura, M., & Mineshige, S. 1997, *PASJ*, 49, 673  
Genzel, R., Weitzel, L., Tacconi-Garman, L. E., Blietz, M., Cameron, M., Krabbe, A., Lutz, D., & Sternberg, A. 1995, *ApJ*, 444, 129  
González Delgado, R. M., Heckman, T., & Leitherer, C. 2001, *ApJ*, 546, 845  
Goodrich, R. W., Veilleux, S., Hill, G. J. 1994, *ApJ*, 422, 521  
Goodrich, R. W. 1995, *ApJ*, 440, 141  
Heckman, T., Blitz, L., Wilson, A., Armus, L., & Miley, G. 1989, *ApJ*, 342, 735  
Heckman, T., Krolik, J., Meurer, G., Calzetti, D., Kinney, A., Koratkar, A., Leitherer, C., Robert, C., Wilson, A. 1995, *ApJ*, 452, 549  
Hill, J. K., Isensee, J. E., Cornett, R. H., Bohlin, R. C., O'Connell, R. W., Roberts, M. S., Smith, A. M., & Stecher, T. P. 1994, *ApJ*, 425, 122  
Hooper, E. J., Impey, C. D., & Foltz, C. B. 1997, *ApJ*, 480, L95  
Hunt, L. K., Malkan, M. A., Salvati, M., Mandolesi, N., Palazzi, E., & Wade, R. 1997, *ApJS*, 108, 229  
Leitherer, C., Vacca, W. D., Conti, P. S., Filippenko, A. V., Robert, C., & Sargent, W. L. W. 1996, *ApJ*, 465, 717  
Kirhakos, S., Bahcall, J. N., Schneider, D. P., & Kristian, J. 1999, *ApJ*, 520, 67  
Krolik, J. H. & Begelman, M. C. 1988, *ApJ*, 329, 702  
Mac Low, M. -M. & McCray, R. 1988, *ApJ*, 324, 776  
Mac Low, M. -M., McCray, R., & Norman, M. L. 1989, *ApJ*, 337, 141  
Manske, V., Henning, Th., & Men'shchikov, A. B. 1998, *A&A*, 331, 52  
McLeod, K. K. & Rieke, G. H. 1995a, *ApJ*, 441, 96  
McLeod, K. K. & Rieke, G. H. 1995b, *ApJ*, 454, L77  
McLure, R. J., Dunlop, J. S., & Kukula, M. J. 2000, *MNRAS*, 318, 693  
McLure, R. J., Kukula, M. J., Dunlop, J. S., Baum, S. A., O'Dea, C. P., & Hughes, D. H. 1999, *MNRAS*, 308, 377  
Maiolino, R., Krabbe, A., Thatte, N., & Genzel, R. 1998a, *ApJ*, 493, 650  
Maiolino, R. & Rieke, G. H. 1995, *ApJ*, 454, 95  
Maiolino, R., Ruiz, M., Rieke, G. H., & Keller, L. D. 1995, *ApJ*, 446, 561  
Maiolino, R., Ruiz, M., Rieke, G. H., & Papadopoulos, P. 1997, *ApJ*, 485, 552  
Maiolino, R., Salvati, M., Bassani, L., Dadina, M., della Ceca, R., Matt, G., Risaliti, G., & Zamorani, G. 1998b, *A&A*, 338, 781  
Malkan, M. A., Gorjian, V., & Tam, R. 1998, *ApJS*, 117, 25  
Maoz, D., Barth, A. J., Sternberg, A., Filippenko, A. V., Ho, L. C., Macchetto, F. D., Rix, H.-W., & Schneider, D. P. 1996, *AJ*, 111, 2248  
Marconi, A., Moorwood, A. F. M., Origlia, L., & Oliva, E. 1994, *ESO Messenger*, 78, 20  
Mathis, J. S., Ruml, W., & Nordsieck, K. H. 1977, *ApJ*, 217, 425  
Matt, G., Fiore, F., Perola, G. C., Piro, L., Fink, H. H., Grandi, P., Matsuoka, M., Oliva, E., & Salvati, M. 1996, *MNRAS*, 281, L69

- Matt, G., Guainazzi, M., Maiolino, R., Molendi, S., Perola, G. C., Antonelli, L. A., Bassani, L., Brandt, W. N., Fabian, A. C., Fiore, F., Iwasawa, K., Malaguti, G., Marconi, A., & Poutanen, J. 1999, *A&A*, 341, L39
- Mauder, W., Weigelt, G., Appenzeller, I., & Wagner, S. J. 1994, *A&A*, 285, 44
- Miller, J. S. & Goodrich, R. W. 1990, *ApJ*, 355, 456
- Miller, J. S., Goodrich, R. W., & Mathews, W. G. 1991, *ApJ*, 378, 47
- Nakamoto, T. & Nakagawa, Y. 1994, *ApJ*, 421, 640
- Neff, S. G., Fanelli, M. N., Roberts, L. J., O'Connell, R. W., Bohlin, R., Roberts, M. S., Smith, A. M., & Stecher, T. P. 1994, *ApJ*, 430, 545
- Norman, C. & Scoville, N. 1988, *ApJ*, 332, 124
- Norman, C. A. & Ikeuchi, S. 1989, *ApJ*, 345, 372
- Ohsuga, K. & Umemura, M. 1999, *ApJ*, 521, L13
- Ohsuga, K., Umemura, M., Fukue, J., & Mineshige, S. 1999, *PASJ*, 51, 345
- Ohta, K., Yamada, T., Nakanishi, K., Kohno, K., Akiyama, M., & Kawabe, R. 1996, *Nature*, 382, 426
- Oliva, E., Marconi, A., & Moorwood, A. F. M. 1999, *A&A*, 342, 87
- Oliva, E., Origlia, L., Kotilainen, J. K., & Moorwood, A. F. M. 1995, *A&A*, 301, 55
- Omont, A., Petitjean, P., Guilloteau, S., McMahan, R. G., Solomon, P. M., & Pecontal, E. 1996, *Nature*, 382, 428
- Pier, E. A., & Krolik, J. H. 1992a, *ApJ*, 399, L23
- Pier, E. A., & Krolik, J. H. 1992b, *ApJ*, 401, 99
- Pier, E. A., & Krolik, J. H. 1993, *ApJ*, 418, 673
- Pérez-Olea, D. E. & Colina, L. 1996, *ApJ*, 468, 191
- Risaliti, G., Maiolino, R., & Salvati, M. 1999, *ApJ*, 522, 157
- Rix, H.-W., Rieke, G., Rieke, M., & Carleton, N. P. 1990, *ApJ*, 363, 480
- Roche, P. F., Aitken, D. K., Smith, C. H., & Ward, M. J. 1991, *MNRAS*, 248, 606
- Rodriguez-Espinosa, J. M., Rudy, R. J., & Jones, B. 1987, *ApJ*, 312, 555
- Rudy, R. J., Cohen, R. D., & Ake, T. B. 1988, *ApJ*, 332, 172
- Schiano, A. V. R. 1985, *ApJ*, 299, 24
- Schinnerer, E., Eckart, A., & Tacconi, L. J. 1998, *ApJ*, 500, 147
- Scoville, N. Z., Sanders, D. B., Sargent, A. I., Soifer, B. T., Scott, S. L., & Lo, K. Y. 1986, *ApJ*, 311, L47
- Scoville, N. Z., Sargent, A. I., Sanders, D. B., & Soifer, B. T. 1991, *ApJ*, 366, L5
- Shapiro, P. R. & Field, G. B. 1976, *ApJ*, 205, 762
- Sherman, R. D. 1979, *ApJ*, 232, 1
- Soifer, B. T., Sanders, D. B., Neugebauer, G., Danielson, G. E., Lonsdale, C. J., Madore, B. F., & Persson, S. E. 1986, *ApJ*, 303, L41
- Storchi-Bergmann, T., Mulchaey, J. S., & Wilson, A. S. 1992, *ApJ*, 395, L73
- Storchi-Bergmann, T., Raimann, D., Bica, E. L. D., & Fraquelli, H. A. 2000, *ApJ*, 544, 747
- Storchi-Bergmann, T., Rodriguez-Ardila, A., Schmitt, H. R., Wilson, A. S., & Baldwin, J. A. 1996, *ApJ*, 472, 83
- Storchi-Bergmann, T., Schmitt, H. R., & Fernandes, R. C. 1999, in *IAU Symposium No. 194, Activity in Galaxies and Related Phenomena*, ed. Y. Terzian, E. Khachikian, & D. Weedman (San Francisco: ASP), 295
- Storchi-Bergmann, T., Wilson, A. S., & Baldwin, J. A. 1996, *ApJ*, 460, 252
- Theis, Ch., Burkert, A., & Hensler, G. 1992, *A&A*, 265, 465
- Tomisaka, K. & Ikeuchi, S. 1986, *PASJ*, 38, 697
- Tomisaka, K. & Ikeuchi, S. 1988, *ApJ*, 330, 695
- Umemura, M., Fukue, J., & Mineshige, S. 1997, *ApJ*, 479, L97
- Umemura, M., Fukue, J., & Mineshige, S. 1998, *MNRAS*, 299, 1123
- Veilleux, S., Cecil, G., Bland-Hawthorn, J., Tully, R. B., Filippenko, A. V., & Sargent, W. L. W. 1994, *ApJ*, 433, 48
- Wilson, A. S., Helfer, T. T., Haniff, C. A., & Ward, M. J. 1991, *ApJ*, 381, 79
- Wilson, A. S., Ward, M. J., & Haniff, C. A. 1988, *ApJ*, 334, 121